

THE STARBURST PROPERTIES OF M82, M83 AND IC342

C. E. Walker,^{1,2}

McDonald Observatory, University of Texas at Austin

F. N. Bash,¹

McDonald Observatory, University of Texas at Austin

R. N. Martin,

Sub-Millimeter Telescope Observatory, University of Arizona

and

T. G. Phillips

Department of Physics, Caltech

RESUMEN

Se usaron las observaciones en líneas moleculares milimétricas y submilimétricas, para sondear el medio interestelar en unos cuantos kpc centrales de tres galaxias con brotes de formación estelar: M82, IC342 y M83. Los medios moleculares asociados con la actividad de formación estelar en estas galaxias parecen estar compuestos de componentes múltiples. Los brotes de formación estelar en M82 y M83 tienen características similares. El brote de formación estelar en IC342 es mucho más moderado, con muchas de las propiedades de la nube similares a aquellas observadas en el kiloparsec central de la Vía Láctea. Se observa una correlación entre el tamaño de la nube y la eficiencia en la formación de las estrellas en cada galaxia; cuanto mayor es la eficiencia, menor es el tamaño de la nube. También parece haber una correlación entre la eficiencia de formación estelar y la densidad superficial del gas ($\sigma_g \propto \epsilon$).

ABSTRACT

Millimeter and submillimeter-wave molecular line observations were used to probe the interstellar medium in the central few kpc of three nearby starburst galaxies: M82, IC342, and M83. The molecular mediums associated with starburst activity in these galaxies appear to be composed of multiple components. The starbursts in M82 and M83 have similar characteristics. The starburst occurring in IC342 is much more subdued, with many of the derived cloud properties similar to that observed in the central kiloparsec of the Milky Way. A correlation is observed between the cloud size and the star formation efficiency in each galaxy; the higher the efficiency, the smaller the cloud size. There also appears to be a correlation between star formation efficiency and gas surface density ($\sigma_g \propto \epsilon$).

Key words: GALAXIES: INDIVIDUAL (M82, M83, IC342) — GALAXIES: INTERSTELLAR MATTER — GALAXIES: STARBURST

¹Visiting Astronomer at the Caltech Submillimeter Observatory which is operated by Caltech under contract to the National Science Foundation

²Visiting Astronomer at the National Radio Astronomy Observatory 12 m telescope which is operated by Associated Universities Inc., under contract to the National Science Foundation

1. INTRODUCTION AND BACKGROUND

Millimeter and submillimeter-wave molecular line observations were used to probe the interstellar medium in the central few kpc of three nearby starburst galaxies: M82, IC342, and M83. Each galaxy was mapped in the $J=3\rightarrow 2$ transition of CO (at the CSO) and the $J=2\rightarrow 1$ transition of CS (at NRAO). M82 was also mapped in the $J=2\rightarrow 1$ transition of CO. Isotopic transitions of CO were observed toward selected positions in each galaxy. $C^{18}O$ $3\rightarrow 2$ emission was detected for the first time toward two positions in M82; CO $4\rightarrow 3$ emission was detected for the first time toward three positions in M83. In addition, high angular resolution 60 and 100 μm *IRAS* images were generated, via a Richardson-Lucy algorithm, and used to study the thermal dust emission in IC342 and M83. A detailed analysis of the molecular gas data was performed using both LTE and non-LTE techniques.

2. RESULTS

Our analysis reveals that a single temperature model for the molecular gas cannot explain the observed line ratios; a multicomponent temperature model is indicated (see Figure 1). Temperatures in the molecular medium in the centers of all three galaxies range from 10 to ≤ 50 K. Main and isotopic line ratios toward IC342 and M83 suggest that the molecular clouds are optically thick and externally heated.

The dust temperatures derived from *IRAS* high resolution images of M83 and IC342 are consistent with those derived from CO and indicate dust and gas temperatures are higher in the nuclei and bars than in the surrounding disks. Elevated dust and gas temperatures (~ 30 to 35 K) are also observed toward HII regions in the disks. The similarity between temperatures derived from the gas and dust suggest densities in the nuclear molecular clouds are $\sim 10^5 \text{ cm}^{-3}$. Such high densities are consistent with the detection of CS towards these regions.

A comparison of ^{12}CO and ^{13}CO observations along the major axis of M82 indicates gas optical depths are highest towards positions $\sim 12''$ northeast and southwest of the $2 \mu m$ peak (see Figure 2). These positions are associated with the molecular ring observed in ^{12}CO . A comparison of ^{13}CO and $C^{18}O$ $J=3\rightarrow 2$ observations towards the central region of M82 reveals that in order for the CO emission to be optically thin (as suggested by the CO main line ratios) the ^{13}CO to $C^{18}O$ abundance ratio must be ~ 3 (see Figure 3).

With half-peak integrated intensity diameters of 630, 1000 and 1300 pc, the derived gas masses, M_g , toward the centers of M82, M83, and IC342 are 5.5×10^7 , 3.5×10^7 , and $6.4 \times 10^7 M_\odot$ respectively. The mass of young stars, M_s , associated with the starburst in each galaxy was estimated from observed luminosities. Using these mass estimates, the star formation efficiency ($\sim M_s/(M_s + M_g)$) was found to be 77, 60, and 10% for M82, M83, and IC342 respectively. Assuming a Salpeter initial mass function, the observed luminosities indicate star formation rates of 16, 6, and $2.5 M_\odot/\text{yr}$ for the three galaxies. Using our gas temperature and density estimates we derived areal and volume filling factors for the molecular medium. These estimates, along with the half-peak integrated intensity diameters, are used to compute the size and number of clouds in the nuclear region of each galaxy. The average cloud sizes are 0.6, ≤ 1 and ≥ 11 pc in M82, M83 and IC342, respectively. Likewise, the corresponding numbers of such clouds in these galaxies are 10^4 , $\geq 10^4$ and ≤ 30 . In addition, the derived values of M_g and the observed size of the emission regions were used to compute the molecular gas surface density towards the nucleus of each source. These surface densities are 174, 140 and $82 M_\odot/\text{pc}^2$ for M82, M83 and IC342, respectively. Table 1 summarizes the values of the parameters discussed above.

3. SUMMARY

1) The molecular mediums associated with starburst activity in M82, M83, and IC342 appear to be composed of multiple components. The temperatures of these components range from 10 to ~ 45 K. Gas densities of $\sim 10^5 \text{ cm}^{-3}$ are indicated.

2) The starbursts in M82 and M83 have similar characteristics. The starburst occurring in IC342 is much more subdued, with many of the derived cloud properties similar to that observed in the central kiloparsec of the Milky Way.

3) A correlation is observed between the cloud size and the star formation efficiency in each galaxy; the higher the efficiency, the smaller the cloud size. Due to the expected instability and resulting short lifetime of small clouds in the turbulent, energetic nuclear regions of starbursts, small clouds appear to be a result and not a cause of high star formation efficiencies.

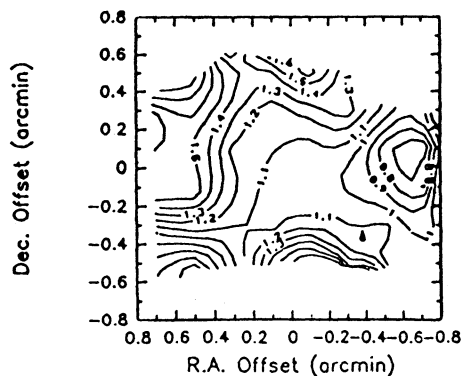


Fig. 1a.

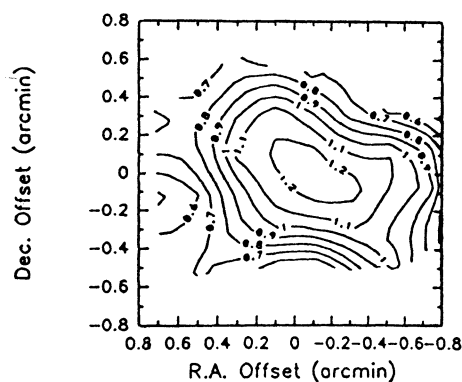


Fig. 1b.

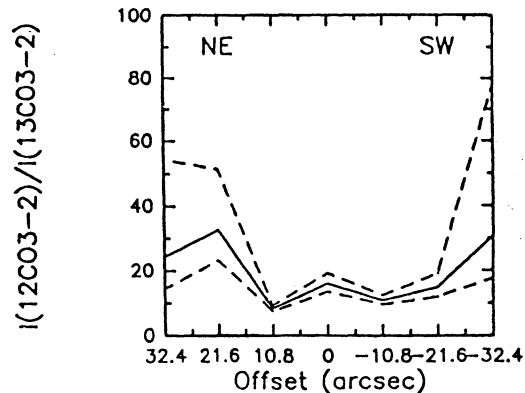


Fig. 2a.

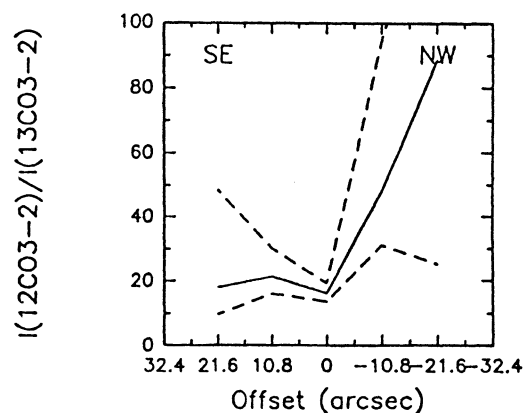


Fig. 2b.

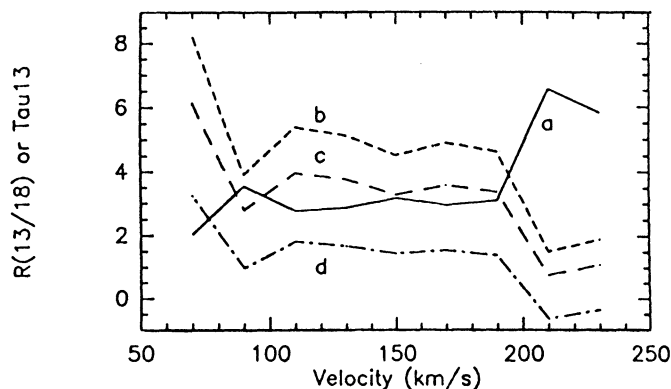


Fig. 3.

Figure 1. Ratio maps of integrated intensity toward M82: a) $\text{CO}(3 \rightarrow 2)/\text{CO}(2 \rightarrow 1)$ and b) $\text{CO}(2 \rightarrow 1)/\text{CO}(1 \rightarrow 0)$. The $\text{CO}(3 \rightarrow 2)$ and $\text{CO}(1 \rightarrow 0)$ data were convolved to the same angular resolution as the $\text{CO}(2 \rightarrow 1)$ data ($31''$). Ratios range from 0.5 to 1.2 in a) and 0.7 to 1.8 in b). Contours are in intervals of 0.1. The $\text{CO}(1 \rightarrow 0)$ data is from Nakai *et al.* 1987, *PASP*, 39, 685.

Figure 2. The integrated intensity ratio of the $^{12}\text{CO}(3 \rightarrow 2)$ to $^{13}\text{CO}(3 \rightarrow 2)$ line along a) M82's major axis and b) M82's minor axis is indicated by the solid line. The dashed lines denote the maximum value of the error bars. Data is sampled every half-beam width ($10.8''$).

Figure 3. a) The integrated intensity ratio of the $^{13}\text{CO}(3 \rightarrow 2)$ to $\text{C}^{18}\text{O}(3 \rightarrow 2)$ line, $R(13/18)$, toward the SW CO peak position is plotted as a function of velocity (solid line). The optical depth, τ , is also plotted as a function of velocity for an abundance of b) 12, c) 9 and d) 5 (dashed lines).

Table 1.[†]
Summary of Derived Properties for M82, M83, IC342 & the Milky Way

Property	M82	M83	IC342	Galactic Center
T_{ex} (K)	≥ 20	≥ 10	≥ 12	~ 50
τ_{co}	~ 1	≥ 3	≥ 17	—
N_{H_2} (cm^{-2})	1×10^{23}	$\geq 1.2 \times 10^{22}$	1.3×10^{24}	—
M_{g} (M_{\odot})	5.5×10^7	$\sim 3.5 \times 10^7$	6.4×10^7	7.9×10^7
f_{A}	0.1	≤ 0.07	0.004	—
f_{V}	1.6×10^{-4}	$\leq 8 \times 10^{-5}$	4.3×10^{-5}	—
d_{CL} (pc)	0.6	≤ 1	≥ 11	20–30
Cloud Num.	10^4	$\geq 10^4$	≤ 30	10
M_{dyn} (M_{\odot})	6.5×10^8	1.3×10^9	7×10^8	7×10^9
$M_{\text{g}}/M_{\text{dyn}}$	0.08	≥ 0.02	0.10	0.01
L_{IR} (L_{\odot})	2.5×10^{10}	9×10^9	3.8×10^9	1×10^9
ϵ (%)	77	60	10	< 2
SFR ($\frac{M_{\odot}}{\text{yr}}$)	16	6	2.5	0.3–0.6
τ_{d} (yr)	3.4×10^6	2.9×10^6	2.6×10^7	3×10^8
D_{E} (pc)	630	1300	1000	1000
σ_{g} ($\frac{M_{\odot}}{\text{pc}^2}$)	174	140	82	101

[†]Description of Table Parameters

T_{ex} = gas excitation temperature (K)

τ_{co} = $^{12}\text{CO}(3 \rightarrow 2)$ tau

N_{H_2} = column density of molecular Hydrogen (cm^{-2})

M_{g} = molecular gas mass within the half intensity region (M_{\odot})

f_{A} = areal filling factor

f_{V} = volume filling factor

d_{CL} = average cloud diameter within the half intensity region (pc)

Cloud Num.= average number of clouds within the half intensity region

M_{dyn} = dynamical mass within the half intensity region (M_{\odot})

$M_{\text{g}}/M_{\text{dyn}}$ = fraction of molecular gas to total (dynamical) mass

L_{IR} = far-infrared luminosity within the half intensity region

ϵ = star formation efficiency as defined by $M_{\text{s}}/(M_{\text{s}}+M_{\text{g}})$ (%); M_{s} = mass of young stars

SFR= star formation rate (M_{\odot}/yr)

τ_{d} = gas depletion timescale (yr)

D_{E} = diameter of the half intensity region (pc)

σ_{g} = molecular gas surface density within the half intensity region (M_{\odot}/pc^2)

4) There appears to be a correlation between star formation efficiency and gas surface density ($\sigma_{\text{g}} \propto \epsilon$). However, no similar trend is found between the total gas mass associated with a starburst and star formation efficiency.

C.E.W. and F.N.B. would like to thank the NRAO and CSO staffs for their support in the data collection and reduction phases of this project. C.E.W. and F.N.B. wish to acknowledge support from the W. M. Keck Foundation.

Frank N. Bash and Constance E. Walker: McDonald Observatory, University of Texas at Austin, Administrative & Research Offices, Austin, TX 78712-1083, U.S.A.

Robert N. Martin: Sub-Millimeter Telescope Observatory, University of Arizona, Tucson, AZ 85721, U.S.A.

Thomas G. Phillips: Caltech, Dept. of Physics MS 320-47, Pasadena, CA 91125, U.S.A.